Spacing-Tailored Multicore Fiber Interface for Efficient FIFO Devices

Ji, Wei; Shen, Zihao; Yu, Ruowei; Wang, Caoyuan; Yan, Zhengyu; Liu, Liying; Xu, Lei; Chen, Wei; Chiang, Kin Seng; Xiao, Limin

Published in:
Journal of Lightwave Technology

Published: 15/08/2022

Document Version:
Post-print, also known as Accepted Author Manuscript, Peer-reviewed or Author Final version

Published version (DOI):
10.1109/JLT.2022.3177622

Publication details:
Ji, W., Shen, Z., Yu, R., Wang, C., Yan, Z., Liu, L., Xu, L., Chen, W., Chiang, K. S., & Xiao, L. (2022). Spacing-Tailored Multicore Fiber Interface for Efficient FIFO Devices. *Journal of Lightwave Technology*, *40*(16), 5682-5688. https://doi.org/10.1109/JLT.2022.3177622

Ji, W., Shen, Z., Yu, R., Wang, C., Yan, Z., Liu, L., Xu, L., Chen, W., Chiang, K. S., & Xiao, L. (2022). Spacing-Tailored Multicore Fiber Interface for Efficient FIFO Devices. *Journal of Lightwave Technology, 40*(16), 5682-5688. https://doi.org/10.1109/JLT.2022.3177622.

Spacing-Tailored Multicore Fiber Interface for Efficient FIFO Devices

Wei Ji, Zihao Shen, Ruowei Yu, Caoyuan Wang, Zhengyu Yan, Liying Liu, Lei Xu, Wei Chen, Kin Seng Chiang, and Limin Xiao

***Abstract*—Multicore fibers (MCFs) have attracted intense attention to overcome the capacity limit of single-core optical fiber communication system. However, as indispensable connection devices between the MCF and the individual single mode fiber (SMF), fan-in and fan-out (FIFO) devices are challenging to achieve overall performance in terms of coupling efficiency, crosstalk, return loss, and device compactness. Here we develop an MCF reverse-tapering technique to increase the core-to-core spacing of the MCF and construct a spacing-tailored interface between the MCF and the normal SMF bundle. The fabricated FIFO device for the small-core MCF with narrow core-to-core spacing of 35 μm features a low average coupling loss (~ 0.6 dB), extraordinarily low crosstalk (< -65 dB) and a return loss (< -60 dB) without using any bridge elements, where the remarkably low crosstalk is about 20 dB lower than using special bridge fibers for the same type of MCF. The flexibility of reverse tapering of MCFs can overcome its intrinsic integration challenge and provide a powerful approach to constructing all-fiber FIFO devices with compact construction and excellent overall performance.**

***Index Terms*—Multicore fibers, fan-in and fan-out devices, space division multiplexing.**

I. Introduction

Multicore fibers (MCFs), due to their high-density multichannel architecture, have been employed in space-division multiplexing telecommunication system [1-3], data center [4-6], 3D shape sensing [7-9], and quantum information processing [10-12] to overcome the limits of conventional single mode fibers (SMFs) and possess great potential in the next generation of telecommunication applications. However, the small core-to-core spacing between the densely packed channels of MCF poses a challenge for low-crosstalk coupling at the fiber interface in the indispensable fan-in and fan-out (FIFO) devices [13]. This is an important topic and various methods such as free-space lens optics [14-18], laminated polymer waveguides [19, 20], 3D laser inscription waveguides [1, 21-23], etched fiber assemblies [24-27], and special bridge fiber bundles [13, 28-32] have been proposed for FIFO devices. Each method has its advantages and drawbacks to achieve the overall performance. The free-space coupling method can achieve low coupling loss (< 0.5 dB), however, the bulky lens system may have drawbacks in device compactness and long-term robustness [14, 15]. The waveguide method can support a scalable solution, however, the relatively high coupling loss (> 2 dB) and high return loss may prevent the utilization in the advanced telecom system which is sensitive to problems of reflection [19, 23]. The etched fiber assemblies can realize compact package and minimum coupling loss ranging from less than 0.3 dB to 2 dB. However, this method can only support the standard core design of MCF and the small core-to-core spacing between the etched SMFs may increase the crosstalk, which will limit the flexible design of MCFs with dense channels [25, 27]. The use of special bridge fiber bundles can provide an all-fiber fused connection, however, MCFs with different parameters will require various designs of bridge fibers, which may not be a cost-effective and general way to solve the challenge of FIFO devices [29, 32]. In short, to match the high-density channels of MCF, all these methods require fabricating dedicated planar or fiber multichannel waveguide structures with the reduced channel-spacing at a tiny interface, which may yield increased crosstalk or return loss. Essentially, the rigid interface of MCF makes it challenging to obtain balanced performance of FIFO in terms of device compactness, coupling efficiency, crosstalk, and return loss.

Here, we propose a fundamentally different new approach,

Manuscript received XX. This work was supported by the Fund of Yiwu Research Institute of Fudan University; and Foundation of the open project of the Shanghai Institute of Optics and Fine Mechanics, Chinese Academy of Science (kjjg-2021-2). *(W. Ji, Z. Shen, R. Yu, and C. Wang contributed equally to this work.) (Corresponding author: Limin Xiao.)*

W. Ji, Z. Shen, R. Yu, C. Wang, Z. Yan, and L. Xiao are with the Advanced Fiber Devices and Systems Group, Key Laboratory of Micro and Nano Photonic Structures (MoE), Key Laboratory for Information Science of Electromagnetic Waves (MoE), Shanghai Engineering Research Center of Ultra-Precision Optical Manufacturing, School of Information Science and Technology, Fudan University, Shanghai, China (e-mail: wji20@fudan.edu.cn; zhshen19@fudan.edu.cn; rwyu20@fudan.edu.cn; cywang18@fudan.edu.cn; zyyan19@fudan.edu.cn; liminxiao@fudan.edu.cn).

L. Liu and L. Xu are with Key Lab for Micro and Nanophotonic Structures (MoE), Department of Optical Science and Engineering, School of Information Science and Engineering, Fudan University, Shanghai, China (e-mail: lyliu@fudan.edu.cn; lei_xu@fudan.edu.cn).

L. Xu is also with the Department of Physics, Fudan University, Shanghai, China.

W. Chen is with Key Laboratory of Specialty Fiber Optics and Optical Access Networks, Joint International Research Laboratory of Specialty Fiber Optics and Advanced Communication, Shanghai University, Shanghai, China. He is also with Jiangsu Hengtong Fiber Science and Technology Corporation, Suzhou, Jiangsu Province, China (e-mail: chenweiSD@shu.edu.cn).

K. S. Chiang is with the Department of Electrical Engineering, City University of Hong Kong, 83 Tat Chee Avenue, Kowloon, Hong Kong SAR, China (e-mail: eeksc@cityu.edu.hk).

L. Xiao is also with Yiwu Research Institute of Fudan University, Chengbei Road, Yiwu, Zhejiang Province, China.

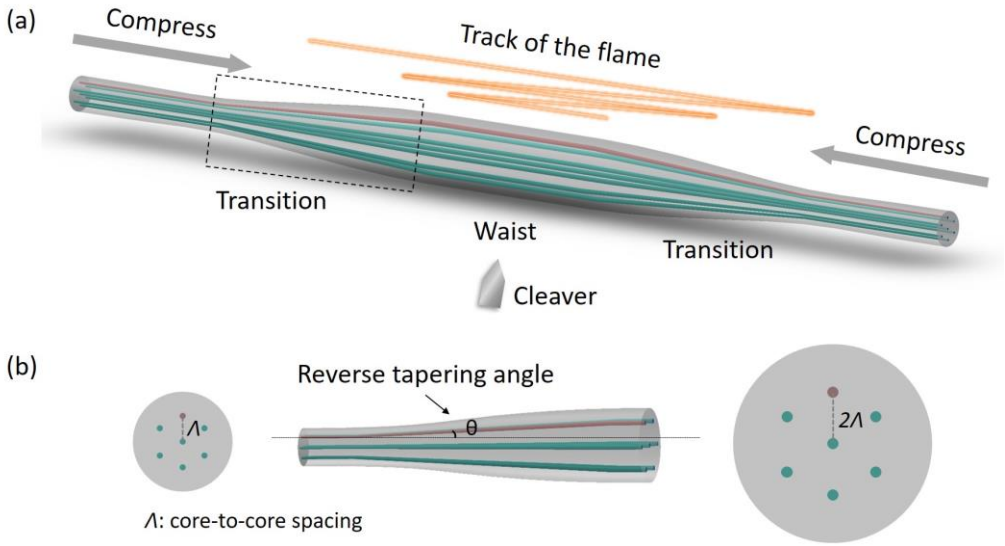

Fig. 1. (a) Schematics of reversely tapering an MCF. (b) Partial enlargement of half of the reverse-tapered MCF with an enlargement ratio of 2, and the two cross sections represent the initial MCF (left) and the reverse-tapered MCF (right).

i.e., MCF reverse tapering, to enabling an efficient-coupling interface of MCF. To the best of our knowledge, reverse tapering has not been applied to an MCF before. We demonstrate tailoring of the channel spacing of MCF, and then construct an all-fiber fused taper type FIFO device without using bridge fiber bundles, which exhibits low average coupling loss (~0.6 dB), and extraordinarily low average crosstalk (<-65 dB) and return loss (<-60 dB). Our new spacing-tailored MCF technique can overcome the intrinsic integration challenge of MCF, facilitates compact and highly efficient FIFO device construction without using any bridge elements, and hence may advance various MCF design and applications.

II. Construction of MCF FI/FO Devices

The key idea of our technique, as illustrated in Fig. 1, is that, the MCF bathed in the flame of a homemade tapering rig is pushed inward precisely from the two ends. The reverse taper consists of a uniform spacing-enlarged multicore waist and two transitions, and the compression process is carefully optimized to ensure adiabatic reverse-tapering with low loss and crosstalk. Subsequently, the cleaved fattened waist can provide an efficient-coupling interface with a larger core-to-core spacing.

To demonstrate the applicability of our technique, two typical types of MCFs, small-core MCF1 from Fibercore (SM-7C1500) and standard-core trench-assisted MCF2 from Hengtong were used. Figs. 2(a, b) show the cross-section images of the two MCFs. The cladding diameter, the core size, the mode field diameter (MFD) at the wavelength of 1550 nm, the core-to-core spacing, and the core positional error of MCF1 are 125 μm, 6.1 μm, 6.4 μm, 35 μm, and 0.57 μm respectively. And the corresponding parameters of MCF2 are 125 μm, 8 μm, 10.4 μm, 37.6 μm, and 1.23 μm, respectively. It should be noted that both of the MCFs used have relatively small core-to-core spacing in the type of weakly-coupled MCFs, which induces the difficulties in fabricating low-crosstalk and efficient FIFO devices.

The construction of an efficient FIFO device means a low

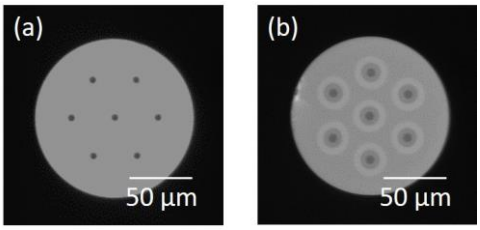

Fig. 2. Cross-section images of (a) small-core MCF1 and (b) normal-core trench-assisted MCF2 at the same scale.

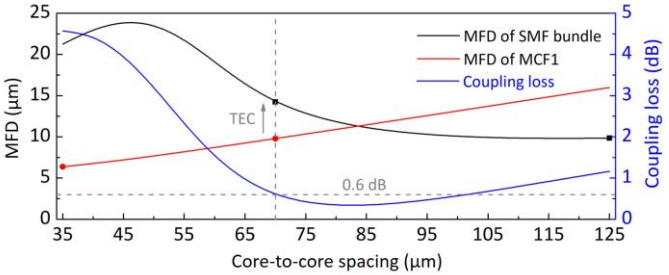

Fig. 3. Variations of the MFD of fundamental mode in SMF bundle and MCF1 with the core-to-core spacing and the corresponding coupling losses between them at the wavelength of 1550 nm.

coupling-loss interface between the SMF bundle and the MCF when the core-to-core spacing is the same. Here we take the MCF1 and the normal Corning SMF-28 bundle as an example to reveal the efficient coupling scheme. Fig. 3 shows the theoretical MFD variations of the fundamental mode in the tapered SMF bundle and the reversely tapered MCF at different core-to-core spacings and the corresponding coupling losses between them at the wavelength of 1550 nm. The calculated coupling loss between the SMF bundle and the spacing-matched MCF1 indicates that the coupling loss can be reduced to less than 0.6 dB when the spacing is in the range from 70 μm to 100 μm, which provides a relatively wide and flexible range for the experimental implementation of a FIFO interface. As shown in Fig. 3, when the spacing increases from the initial 35 μm to 70 μm (red dots in the curve) for the reverse-tapered MCF1(reverse tapering ratio of 2), the core size increases from

6.1 μm to 12.2 μm, and the calculated MFD [33] is enlarged from 6.4 μm to 10 μm. For the down-tapered SMF bundle, when the spacing decreases from the initial spacing of 125 μm to 70 μm (black squares in the curve), the calculated MFD is enlarged from 10 μm to 14 μm, achieving a theoretical coupling loss of 0.59 dB. We can find the taper with the larger spacing of 84 μm (ratio of 2.38) may achieve a little bit lower coupling loss as illustrated in Fig. 3. However, in the experiment, we chose the reverse taper with the outer diameter of 250 μm (the ratio of 2) for mode-matching since the taper with the outer diameter of 250 μm is much easier to be cleaved compared with those with larger outer diameters using the cleaver Fujikura CT-100. Indeed, a high-quality cleaved MCF taper with a flat end-facet is significantly important to support a low-loss splicing in the next step. In this case, the thermally expanded core (TEC) process [34, 35] can be used to increase the MFD of tapered MCF1 and improve the mode matching further.

The reverse tapering process of MCFs was implemented. A section of MCF with the jacket was firstly stripped off and cleaned. Then it was firmly held between two vacuum chucks that had been precisely aligned. The bare section of MCF was heated in an oxy-hydrogen flame by a flame brush technique, and it was bulged with the gradual pushing from the two sides. The final waist diameter is determined by the length of the heating zone, the initial fiber diameter, the pushing distance [33]. By controlling these parameters, we can enlarge the MCF diameter and thus increase its core-to-core spacing to match with that of the tapered SMF bundle. It is crucial that the MCF was located in the uniform temperature region of a wide flame, and care should be taken when locating the MCF in the flame by adjusting the flame position and height; and real-time feedback for loss measurement was used to optimize the fiber pushing rate and flame sweep parameters. We found that uneven heating or improper compression speed during the reverse tapering process induced the multicore spacing distortion or fiber bending. Unlike a single SMF reverse-taper [34, 35], the position of each core should be precisely retained simultaneously during reverse tapering. Besides, the outer channels in the tapered MCF have a small titling angle, as illustrated in Fig. 1(b), and thus it is essential to increase the reverse transition length by varying the flame scanning length during the flame brush process to minimize the macrobending losses of the outer channels. In our experiment, the fiber pushing velocity was 120 μm/s, while the flame sweeping width decreased from 3000 μm to 2000 μm during the sweeping process, and the flame sweeping velocity was adopted as 1000 μm/s. The ultimate core-to-core spacing of the reverse-tapered MCF also depends on the compressing distance, which was about 9000 μm when the enlargement ratio was 2. Care should be taken during the whole reverse tapering process, and we noticed that monitoring the reverse-tapering loss of two channels was a good strategy to obtain the proper fabrication parameters.

The extra loss and crosstalk induced by the MCF reverse tapering process was monitored. We found that they were highly relevant with the physical properties of the transitions, such as the transition length and the local taper angle. The theoretic adiabatic transition length is around 1 mm. When the enlargement ratio was around 2 and the transition length was larger than 6 mm, the reverse tapering loss of each channel was less than 0.1 dB without high-order mode excitation and extra crosstalk. However, a shorter transition length of 1.2 mm will bring a relatively large local taper angle of ~3.4°, causing macrobending losses in outer channels, about 1 dB larger than that in the center core.

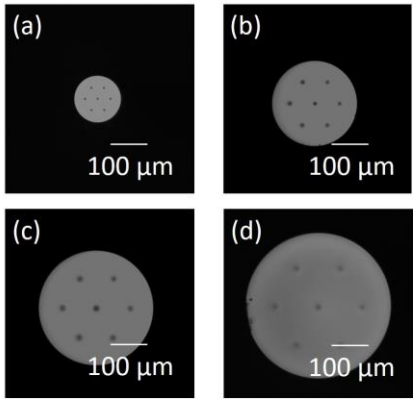

Fig. 4. Microscopic images of (a) initial MCF1 with core-to-core spacing of 35 μm and (b-d) reverse-tapered MCF1 with enlarged spacings of 70, 100, and 125 μm respectively (at the same scale), and the reverse-tapered MCF1(b) with the tailored spacing of 70 μm was used to construct the FIFO device.

After the reverse tapering process, the fattened waist region was cleaved to provide an efficient interface for the FI/FO device. A tension-scribe cleaver (Fujikura CT-100) was used to cleave in the waist region, and different tension values of around 650 g were carefully adjusted to achieve an end-face angle of smaller than 0.2° for the further splicing experiment. It should be noted that a relatively long fattened waist length, i.e., larger than 500 μm, might be necessary to obtain a flat cleaved end face. Figs. 4(b-d) show the microscopic cross-sections of the produced reverse-tapered MCF1, with spacing of 70, 100 and 125 μm, respectively, whose initial spacing was 35 μm (Fig. 4(a)). These flexibly tailored MCF interfaces in Fig. 4 show the capability of controllable matching of core-to-core spacing with that of different SMF bundles. As mentioned in the mode-matching discussion, the MCF1 with the tailored spacing of 70 μm was used to splice with the tapered SMF bundle. When the spacing of the normal SMF tapered bundle is large, i.e., 70 μm, it can still be matched with the reverse tapered MCF interface, indicating that the normal SMF bundle can be directly used to implement the FIFO device without using any special designed SMFs or bridge fibers. It is evident that the enlarged spacing of each channel at the coupling interface will significantly reduce the possibility of crosstalk induced by the positional or alignment errors during connection, which is confirmed by the following experiments.

The modal properties of the reverse-tapered MCF and the tapered SMF bundle were characterized. The normal SMF bundle was down-tapered to form a fused taper type bundle, which was produced by the tapering rig with seven SMF-28 (Corning) fibers inside a fused silica capillary. The initial SMF bundle has an MFD of 10.4 μm and a spacing of 125 μm. Normally, when reducing the spacing to less than 60 μm, the

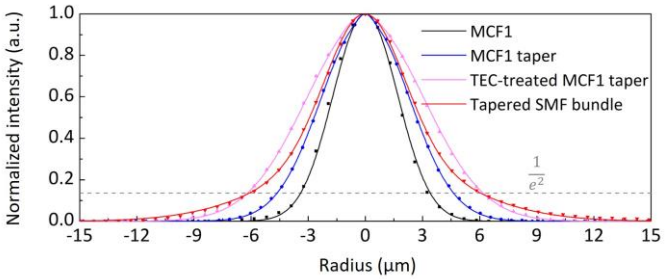

Fig. 5. Normalized intensity profiles of the initial MCF1, and the reverse-tapered MCF1, the TEC-treated reverse-tapered MCF1, and the tapered SMF bundle with a matched spacing of 70 μm.

down-tapered SMF bundle cannot achieve low-crosstalk propagation, and hence specially designed bridge fiber bundles have to be used [29] when connected to different MCFs. However, by using our reverse-tapered MCF interface, the SMF bundle can be down-tapered with a much less extent, avoiding significantly changing the MFD and the crosstalk.

To characterize the variation of MFD of the reverse-tapered MCF and the down-tapered SMF bundle, a measurement system that consisted of an infrared laser source centered at the wavelength of 1550 nm and a modified microscope system with an infrared camera (Xeva XC-130) was adopted [34, 35]. The laser was injected into the untreated end of the tested fiber, and the mode pattern at the treated end was captured. Fig. 5 shows the normalized intensity profiles of the initial MCF1, and the reverse-tapered MCF1, the TEC-treated reverse-tapered MCF1, and the tapered SMF bundle with a matched spacing of 70 μm. When the bundle was tapered down to a spacing of 70 μm, the core size was tapered to 4.6 μm, and the measured MFD ($1/e^2$-intensity) of each core of SMF bundle slightly increased to 12 μm without extra crosstalk. Therefore, when the MCF spacing was reversely tailored to the same value of 70 μm (reverse tapering ratio of 2 for MCF1 and 1.86 for MCF2), the core size was 12.2 μm for MCF1 and 14.9 μm for MCF2; the measured MFD increased from 6.4 μm to 11.0 μm for MCF1, and from 10.4 μm to 13.9 μm for MCF2, indicating that the spacing-tailored MCF are advantageous for direct coupling to the normal tapered SMF bundle. The coupling losses in the MCF/SMF bundle interfaces are estimated to be less than 0.1 dB when only considering the MFD matching [36]. However, other factors such as the mismatch of mode shape and the positional error may also increase the whole coupling loss. In principle, the core size and the core-to-core spacing are enlarged in the same ratio during the reverse tapering [34, 35], however, the increased value of spacing is much larger than that of MFD in this process, which can reduce the mode mismatching while achieving the spatial positional matching. For example, when the core-to-core spacing of MCF1 increases from 35 μm to 70 μm with the increased value of 35 μm, the core size increases from 6.1 μm to 12.2 μm, with an increase of 6.1 μm, while the measured MFD increases from 6.4 μm to 11.0 μm, with the increased value of 4.6 μm only. Furthermore, for the small-core MCF1, the extra TEC technique [34, 35] was used, and the measured MFD of the TEC-treated reverse-tapered MCF1 was modified to 12 μm, improving mode-matching with the SMF bundle. It should be noted that the key advantage of this technique is that the core-to-core spacing and the MFD of MCF can be flexibly tailored, enhancing isolation of individual channels and giving the extra space to modify the MFD without increasing crosstalk, which is unfeasible for a rigid MCF interface.

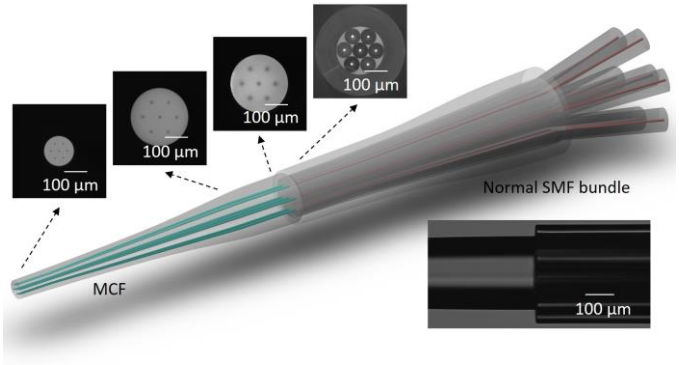

Fig. 6. A splice between a reverse-tapered MCF and an SMF-28 bundle. The upper insets from left to right are the initial MCF1, the reverse-tapered MCF1, the reverse-tapered and TEC-treated MCF1, the tapered SMF-28 bundle, respectively, and the bottom inset is the experimental fused joint.

We then implemented the experiment to construct the all-fiber FI/FO device using the reverse-tapered MCF. Fig. 6 shows a splice between a reverse-tapered MCF1 and an SMF-28 bundle. The schematics illustrates the reverse-tapered MCF1 from the untreated end to the fattened waist through the reverse transition, which is spliced to the tapered SMF bundle. The upper insets from left to right are the experimental cross-sections of the initial MCF1, the reverse-tapered MCF1, the reverse-tapered and TEC-treated MCF1, and the tapered SMF-28 bundle, respectively. The splicing experiment was conducted by the commercial splicer Vytran GPX3400. We first loaded the reverse-tapered MCF and the SMF bundle on the fiber hold blocks, and then observed end-faces of both fibers via the mirror and the imaging system of Vytran. The lateral and rotational alignment functions were used to align cores of the reverse-tapered MCF and the SMF bundle. To further improve the alignment accuracy and balance the coupling efficiency of multichannels, manual alignment was then used by monitoring the coupling losses in the central core and outer cores. Since a wider filament zone is beneficial to the uniform heating for the reverse-tapered MCFs and the SMF bundles with large diameters, a graphite filament FTAV5 was used. The splicing power and the fusion time were optimized to be 135 W and 1.5 s, respectively. Besides, an axial offset in the SMF bundle was set as 30 μm to ensure an almost equivalent heating condition for the two sides due to the larger size of the bundle. As shown in the bottom inset of Fig. 6, a low-loss and robust splicing joint was formed to construct a highly efficient FI/FO device.

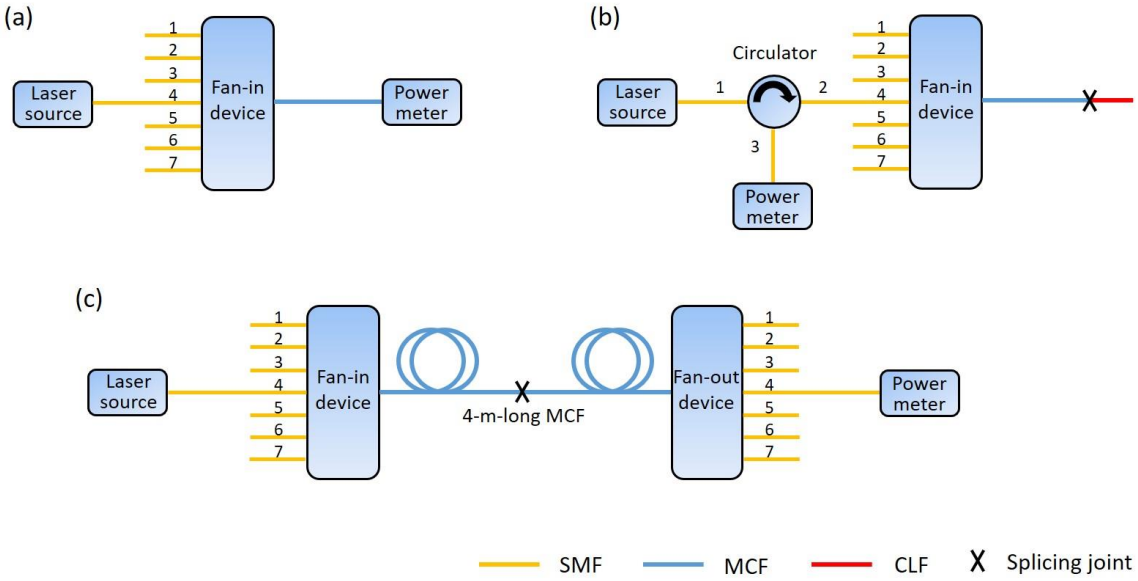

Fig. 7. Schematics of the experimental setup for the measurement of (a) the insertion loss and (b) the return loss for a single FI/FO device, and (c) the crosstalk for a FIFO device.

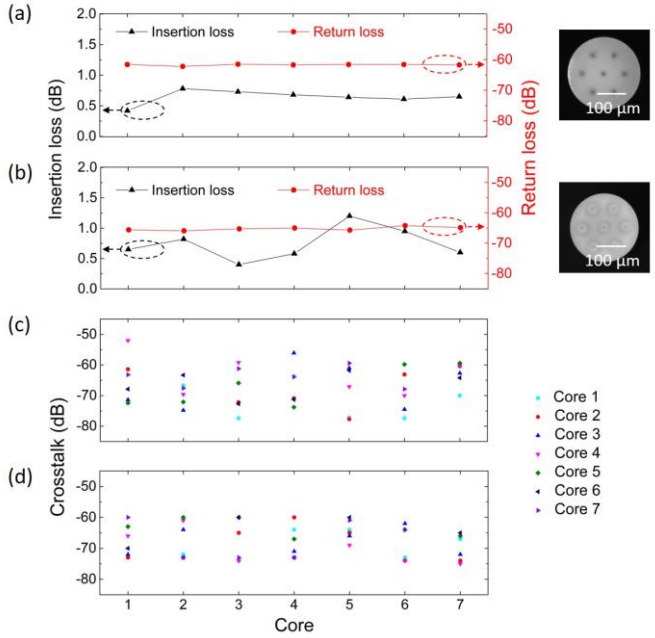

Fig. 8. (a, b) Insertion loss and return loss of the fabricated FIFO device and (c, d) crosstalk of the FIFO for MCF1 and MCF2 respectively. The insets from top to bottom are the cross sections of the reverse-tapered MCF1 and MCF2.

III. Characterization of MCF FIFO Devices

The optical properties of the fabricated MCF FIFO devices were characterized, and the schematics is illustrated in Fig. 7. For a single FI/FO device, as shown in Fig. 7(a), the insertion loss was measured with an infrared laser source centered at the wavelength of 1550 nm and an optical power meter, whose value was defined as the ratio between the output power and the input power for an excited core [15, 25, 29]. As shown in Fig. 7(b), the laser source, the input end of the FI/FO device, and the power meter were connected to a three-port circulator to measure the return loss, and a 1-m-long coreless fiber (CLF) was spliced to the output end of the FI/FO device to minimize the reflection effect of the end of MCF, which was smaller than -65 dB [37]. Figs. 8(a, b) show the measured insertion and return losses of the FI/FO devices we fabricated. For MCF1 and MCF2 at the wavelength of 1550 nm, the insertion losses were about 0.64±0.11 dB and 0.74±0.27 dB and the average return losses were lower than -61 dB and -65 dB, respectively. The slightly larger variation in coupling loss of MCF2 may be due to the larger initial core positional error (1.23 μm) of the MCF2 fiber itself.

A pair of FI and FO assemblies was fusion spliced to form an all-fiber MCF FIFO devices with a 4-m-long MCF using Vytran GPX3400 (Fig. 7(c)). After several trials, the splicing parameters between the same MCF were set as the splicing power 120 W and the fusion time 12 s. The average insertion loss of each core for the MCF1-MCF1 splice was 0.13 ± 0.05 dB after measuring each channel, and that for the MCF2-MCF2 splice was 0.07± 0.06 dB. And then the crosstalk for a FIFO device could be measured by exciting each individual core in a FI device and detecting the output power of the other cores in a FO device (Fig. 7(c)) [14, 27, 31]. Fig. 8(c) shows the measured crosstalk of all channels in a FIFO device with 4-m-long MCF1. A remarkably low average crosstalk of -66 dB was confirmed, which is about 20 dB lower than that using special bridge fibers for the same MCF1 [32]. Fig. 8(d) shows the average FIFO crosstalk of -67.5 dB for MCF2. Low FIFO crosstalk was confirmed in these two types of MCFs. Therefore, we have demonstrated the flexibility of our approach to fabricating FIFO devices for different types of weakly-coupled MCFs. Since the mode matching scheme on the MCF/SMF bundle (Fig. 3) reveals the MFD of the tapered normal SMF bundle can be enlarged to a large value within a wide range of core-to-core spacing, our approach can also be used for the strongly-coupled MCFs with closer cores and larger mode sizes. The reverse

tapering ratios for the MCFs can be tailored, enabling the mode matching between the strongly-coupled MCF and the tapered SMF bundle, however, the optimized tapering ratio to reduce the crosstalk should be further investigated.

IV. Conclusions

In conclusion, we have demonstrated a flexible spacing-tailored reverse-tapering approach to fabricating efficient-coupling interfaces of MCFs. Via this powerful technique, the MCF spacing can be significantly enlarged with low loss and crosstalk through the adiabatic reverse-tapering transition. Without using any special bridge fibers, our technique offers a compact architecture to realize highly efficient all-fiber FIFO devices with extraordinarily low crosstalk and return loss. For a small-core MCF with the spacing of 35 μm, the average insertion loss was about 0.64 dB, the average return loss was lower than -61 dB, and the average crosstalk was -66 dB. For a standard-core MCF, the corresponding measurement results are 0.74 dB, -65 dB, and -67.5 dB, respectively. The spacing-tailored interface can release the design constraints of high-density weakly- coupled MCF and facilitate the interconnection between MCFs and other photonic elements. Our approach may also benefit the FIFO devices for the strongly-coupled MCF with smaller spacing and the MCF with more channels due to the ability to tailoring the spacing of MCFs.

References

[1] R. G. Van Uden, R. A. Correa, E. A. Lopez, F. Huijskens, C. Xia, G. Li, A. Schülzgen, H. De Waardt, A. Koonen, and C. M. Okonkwo, "Ultra-high-density spatial division multiplexing with a few-mode multicore fibre," *Nat. Photonics*, vol. 8, no. 11, pp. 865-870, Oct. 2014.

[2] A. Turukhin, O. V. Sinkin, H. Batshon, H. Zhang, Y. Sun, M. Mazurczyk, C. R. Davidson, J.-X. Cai, M. A. Bolshtyansky, and D. G. Foursa, "105.1 Tb/s power-efficient transmission over 14,350 km using a 12-core fiber," presented at the 2016 Optical Fiber Communications Conference and Exhibition (OFC), Anaheim, CA, USA, 2016, Paper Th4C.1.

[3] A. Turukhin, M. Paskov, M. V. Mazurczyk, W. W. Patterson, H. Batshon, O. V. Sinkin, M. A. Bolshtyansky, B. Nyman, D. G. Foursa, and A. N. Pilipetskii, "Demonstration of potential 130.8 Tb/s capacity in power-efficient SDM transmission over 12,700 km using hybrid micro-assembly based amplifier platform," presented at the 2019 Optical Fiber Communications Conference and Exhibition (OFC), San Diego, CA, USA, 2019, Paper M2I.4.

[4] R. Lin, J. Van Kerrebrouck, X. Pang, M. Verplaetse, O. Ozolins, A. Udalcovs, L. Zhang, L. Gan, M. Tang, and S. Fu, "Real-time 100 Gbps/λ/core NRZ and EDB IM/DD transmission over multicore fiber for intra-datacenter communication networks," *Opt. Express*, vol. 26, no. 8, pp. 10519-10526, Apr. 2018.

[5] H. Yuan, M. Furdek, A. Muhammad, A. Saljoghei, L. Wosinska, and G. Zervas, "Space-division multiplexing in data center networks: on multi-core fiber solutions and crosstalk-suppressed resource allocation," *J. Opt. Commun. Netw.*, vol. 10, no. 4, pp. 272-288, Apr. 2018.

[6] R. A. Dias, J. L. Rebola, and A. V. Cartaxo, "Performance analysis of PAM4 signal transmission in inter-datacenter multicore fiber links impaired by inter-core crosstalk," in *Proceedings of the International Conference of Photonics, Optics and Laser Technology (Photooptics)*, Vienna, Austria, 2021, pp. 94-103.

[7] E. M. Lally, M. Reaves, E. Horrell, S. Klute, and M. E. Froggatt, "Fiber optic shape sensing for monitoring of flexible structures," in *Proceedings of SPIE, Sensors and Smart Structures Technologies for Civil, Mechanical, and Aerospace Systems 2012*, San Diego, California, USA, 2012, vol. 8345, p. 83452Y.

[8] Z. Zhao, M. A. Soto, M. Tang, and L. Thévenaz, "Distributed shape sensing using Brillouin scattering in multi-core fibers," *Opt. Express*, vol. 24, no. 22, pp. 25211-25223, Oct. 2016.

[9] T. Kremp, K. S. Feder, W. Ko, and P. S. Westbrook, "Performance characteristics of continuous multicore fiber optic sensor arrays," in *Proceedings of SPIE, Optical Fibers and Sensors for Medical Diagnostics and Treatment Applications XVII*, San Francisco, California, USA, 2017, vol. 10058, p. 100580V.

[10] J. Dynes, S. Kindness, S.-B. Tam, A. Plews, A. Sharpe, M. Lucamarini, B. Fröhlich, Z. Yuan, R. Penty, and A. Shields, "Quantum key distribution over multicore fiber," *Opt. Express*, vol. 24, no. 8, pp. 8081-8087, Apr. 2016.

[11] Y. Ding, D. Bacco, K. Dalgaard, X. Cai, X. Zhou, K. Rottwitt, and L. K. Oxenløwe, "High-dimensional quantum key distribution based on multicore fiber using silicon photonic integrated circuits," *npj Quantum Inform.*, vol. 3, no. 1, pp. 1-7, Jun. 2017.

[12] C. Cai, Y. Sun, Y. Zhang, P. Zhang, J. Niu, and Y. Ji, "Experimental wavelength-space division multiplexing of quantum key distribution with classical optical communication over multicore fiber," *Opt. Express*, vol. 27, no. 4, pp. 5125-5135, Nov. 2019.

[13] B. Zhu, T. Taunay, M. Yan, J. Fini, M. Fishteyn, E. Monberg, and F. Dimarcello, "Seven-core multicore fiber transmissions for passive optical network," *Opt. Express*, vol. 18, no. 11, pp. 11117-11122, May 2010.

[14] J. Sakaguchi, B. J. Puttnam, W. Klaus, Y. Awaji, N. Wada, A. Kanno, T. Kawanishi, K. Imamura, H. Inaba, and K. Mukasa, "305 Tb/s space division multiplexed transmission using homogeneous 19-core fiber," *J. Lightwave Technol.*, vol. 31, no. 4, pp. 554-562, Feb. 2012.

[15] Y. Tottori, H. Tsuboya, T. Kobayashi, and M. Watanabe, "Integrated optical connection module for 7-core multi-core fiber and 7 single mode fibers," presented at the 2013 IEEE Photonics Society Summer Topical Meeting Series, Waikoloa, HI, USA, 2013, Paper MC3.2.

[16] O. Shimakawa, H. Arao, M. Harumoto, T. Sano, and A. Inoue, "Compact multi-core fiber fan-out with GRIN-lens and micro-lens array," presented at the Optical Fiber Communication Conference 2014, San Francisco, California, USA, 2014, Paper M3K.1.

[17] J. Sakaguchi, W. Klaus, J. M. D. Mendinueta, B. J. Puttnam, R. S. Luís, Y. Awaji, N. Wada, T. Hayashi, T. Nakanishi, and T. Watanabe, "Large spatial channel (36-core×3 mode) heterogeneous few-mode multicore fiber," *J. Lightwave Technol.*, vol. 34, no. 1, pp. 93-103, Jan. 2015.

[18] K. Igarashi, D. Soma, Y. Wakayama, K. Takeshima, Y. Kawaguchi, N. Yoshikane, T. Tsuritani, I. Morita, and M. Suzuki, "Ultra-dense spatial-division-multiplexed optical fiber transmission over 6-mode 19-core fibers," *Opt. Express*, vol. 24, no. 10, pp. 10213-10231, May 2016.

[19] T. Watanabe, M. Hikita, and Y. Kokubun, "Laminated polymer waveguide fan-out device for uncoupled multi-core fibers," *Opt. Express*, vol. 20, no. 24, pp. 26317-26325, Nov. 2012.

[20] T. Watanabe, M. Hikita, and Y. Kokubun, "19-core fan-in/fan-out waveguide device for dense uncoupled multi-core fiber," presented at the 2013 IEEE Photonics Conference, Bellevue, WA, USA, 2013, Paper TUG2.4.

[21] R. R. Thomson, H. T. Bookey, N. D. Psaila, A. Fender, S. Campbell, W. N. Macpherson, J. S. Barton, D. T. Reid, and A. K. Kar, "Ultrafast-laser inscription of a three dimensional fan-out device for multicore fiber coupling applications," *Opt. Express*, vol. 15, no. 18, pp. 11691-11697, Sept. 2007.

[22] R. Thomson, R. Harris, T. Birks, G. Brown, J. Allington-Smith, and J. Bland-Hawthorn, "Ultrafast laser inscription of a 121-waveguide fan-out for astrophotonics," *Opt. Lett.*, vol. 37, no. 12, pp. 2331-2333, Jun. 2012.

[23] R. Ryf, N. K. Fontaine, M. Montoliu, S. Randel, S. Chang, H. Chen, S. Chandrasekhar, A. H. Gnauck, R.-J. Essiambre, and P. J. Winzer, "Space-division multiplexed transmission over 3×3 coupled-core multicore fiber," presented at the Optical Fiber Communication Conference 2014, San Francisco, California, USA, 2014, Paper Tu2J.4.

[24] O. Shimakawa, M. Shiozaki, T. Sano, and A. Inoue, "Pluggable fan-out realizing physical-contact and low coupling loss for multi-core fiber," presented at the Optical Fiber Communication Conference 2013, Anaheim, California, USA, 2013, Paper OM3I. 2.

[25] B. Li, Z. Feng, M. Tang, Z. Xu, S. Fu, Q. Wu, L. Deng, W. Tong, S. Liu, and P. P. Shum, "Experimental demonstration of large capacity WSDM optical access network with multicore fibers and advanced modulation formats," *Opt. Express*, vol. 23, no. 9, pp. 10997-11006, May 2015.

[26] M. Yoshida, T. Hirooka, and M. Nakazawa, "Fused type fan-out device for multi-core fiber based on bundled structure," presented at the Optical Fiber Communication Conference 2016, Anaheim, California, USA, 2016, Paper Tu3I.2.

[27] M. Yoshida, T. Hirooka, and M. Nakazawa, "Low-loss and reflection-free fused type fan-out device for 7-core fiber based on a bundled structure," *Opt. Express*, vol. 25, no. 16, pp. 18817-18826, Aug. 2017.
[28] B. Zhu, T. Taunay, M. Fishteyn, X. Liu, S. Chandrasekhar, M. Yan, J. Fini, E. Monberg, and F. Dimarcello, "112-Tb/s space-division multiplexed DWDM transmission with 14-b/s/Hz aggregate spectral efficiency over a 76.8-km seven-core fiber," *Opt. Express*, vol. 19, no. 17, pp. 16665-16671, Aug. 2011.
[29] L. Gan, J. Zhou, L. Shen, X. Guo, Y. Wang, C. Yang, W. Tong, L. Xia, S. Fu, and M. Tang, "Ultra-low crosstalk fused taper type fan-in/fan-out devices for multicore fibers," presented at the 2019 Optical Fiber Communications Conference and Exhibition (OFC), San Diego, CA, USA, 2019, Paper Th3D.3.
[30] Y. Kang, X. Guo, L. Gan, L. Shen, C. Yang, R. Zhang, L. Shen, W. Tong, S. Fu, and M. Tang, "Broadband low-loss fan-in/fan-out devices for multicore fibers," presented at the Asia Communications and Photonics Conference (ACPC) 2019, Chengdu, China, 2019, Paper T1A.4.
[31] J. C. Alvarado-Zacarias, J. E. Antonio-Lopez, M. S. Habib, S. Gausmann, N. Wang, D. Cruz-Delgado, G. Li, A. Schülzgen, A. Amezcua-Correa, and L.-A. Demontmorillon, "Low-loss 19 core fan-in/fan-out device using reduced-cladding graded index fibers," presented at the Optical Fiber Communication Conference 2019, San Diego, California, USA, 2019, Paper Th3D. 2.
[32] V. Kopp, J. Park, J. Singer, D. Neugroschl, and A. Gillooly, "Low return loss multicore fiber-fanout assembly for SDM and sensing applications," presented at the Optical Fiber Communication Conference (OFC) 2020, San Diego, California, USA, 2020, Paper M2C. 3.
[33] M. Artiglia, G. Coppa, P. D. Vita, M. Potenza, and A. Sharma, "Mode field diameter measurements in single-mode optical fibers," *J. Lightwave Technol.*, vol. 7, no. 8, pp. 1139-1152, Aug. 1989.
[34] R. Yu, C. Wang, F. Benabid, K. S. Chiang, and L. Xiao, "Robust mode matching between structurally dissimilar optical fiber waveguides," *ACS Photonics*, vol. 8, no. 3, pp. 857-863, Feb. 2021.
[35] C. Wang, R. Yu, B. Debord, F. Gérôme, F. Benabid, K. S. Chiang, and L. Xiao, "Ultralow-loss fusion splicing between negative curvature hollow-core fibers and conventional SMFs with a reverse-tapering method," *Opt. Express*, vol. 29, no. 14, pp. 22470-22478, Jul. 2021.
[36] L. Xiao, M. S. Demokan, W. Jin, Y. Wang, and C.-L. Zhao, "Fusion splicing photonic crystal fibers and conventional single-mode fibers: Microhole collapse effect," *J. Lightwave Technol.*, vol. 25, no. 11, pp. 3563-3574, Nov. 2007.
[37] P. Wysocki, G. Jacobovitz-Veselka, D. Gasper, S. Kosinski, J. Costelloe, and S. Granlund, "Modeling, measurement, and a simple analytic approximation for the return loss of erbium-doped fiber amplifiers," *IEEE Photon. Technol. Lett.*, vol. 7, no. 12, pp. 1409-1411, Dec. 1995.

Wei Ji received the B.S. degree in photoelectric information science and engineering from China University of Mining and Technology, Xuzhou, China. He is currently working toward the M.S. degree in optical engineering with Fudan University, Shanghai, China. His research interests include multicore fibers and optical fiber devices.

Zihao Shen received the B.S. degree in electronic science and technology from Shandong University, Jinan, China. He is currently working toward the M.S. degree in optical engineering with Fudan University, Shanghai, China. His research interests include multicore fibers and optical fiber sensors.

Ruowei Yu received the B.S. degree in photoelectric information science and engineering from the Nanjing University of Aeronautics and Astronautics, Nanjing, China. She is currently working toward the Ph.D. degree in optical engineering with Fudan University, Shanghai, China. Her research interests include hollow-core photonic crystal fiber technology and all-fiber devices.

Caoyuan Wang received the B.S. degree in photoelectric information science and engineering from the Central South University, Changsha, China. He is currently working toward the Ph.D. degree in optical engineering with Fudan University, Shanghai, China. His research interests include hollow-core photonic crystal fiber technology, all-fiber devices, and fiber sensors.

Zhengyu Yan received the B.S. degree in electronic science and technology and the M.S. degree in optical engineering from Shandong University, Jinan, China. He is currently working toward the Ph.D. degree in optical engineering with Fudan University, Shanghai, China. His research interests include optical fiber sensors and laser technology.

Liying Liu received the B.S. and Ph.D. degrees from Fudan University, Shanghai, China, in 1986 and 1992, respectively. She is a Professor in the Department of Optical Science and Engineering, Fudan University, Shanghai, China. Her research interests include materials and devices for integrated optics, nonlinear optics, and electro-optical devices.

Lei Xu received the B.S. and Ph.D. degrees from Fudan University, Shanghai, China, in 1984 and 1990, respectively. He is currently a Professor in the Department of Optical Science and Engineering, Fudan University, Shanghai, China. His research interests include optical microcavity devices and applications and novel nonlinear optical responses of advanced materials.

Wei Chen is a professor of Shanghai University. He graduated from Huazhong University of Science and Technology in 2011 with the Ph.D. degree in optical engineering. He studied in Harbin University of Science and Technology from 1994 to 2001 and obtained a Bachelor's degree in 1998 and a Master's degree in 2001. From 2001 to 2014, he has worked in Fiberhome Telecommunication Technology Co., Ltd. and from May 2014 to August 2021 in Hengtong Optical Fiber Technology Co., Ltd. He has been mainly engaging in the research of optical fiber communication, specialty optical fiber and fiber sensing technology, and optical fiber devices.

Kin Seng Chiang (M'94) received the B.E. (Hons. I) and Ph.D. degrees in electrical engineering from the University of New South Wales, Sydney, NSW, Australia, in 1982 and 1986, respectively. In 1986, he spent six months with the Department of Mathematics, Australian Defense Force Academy, Canberra, ACT, Australia. From 1986 to 1993, he was with the Division of Applied Physics, Commonwealth Scientific and Industrial Research Organization, Sydney, NSW, Australia. From 1987 to 1988, he spent six months with the Electrotechnical Laboratory, Tsukuba City, Tsukuba, Japan. From 1992 to 1993, he worked concurrently with the Optical Fibre Technology Centre, University of Sydney. In August 1993, he joined the Department of Electronic Engineering, City University of Hong Kong, Kowloon Tong, Hong Kong, where he is currently a Chair Professor. From 2007 to 2010, he was concurrently a Chang Jiang Chair Professor with the University of Electronic Science and Technology of China (UESTC) and is currently associated with UESTC under the National Thousand Talents Program. He has authored or coauthored more than 500 papers on optical fiber/waveguide theory and modeling, fiber/waveguide characterization, fiber/waveguide devices, optical sensors, optical interconnect, and nonlinear guided-wave optics. He served as an Associate Editor for the Journal of Lightwave Technology during 2009–2014, and is currently an Editor for the Light: Science and Applications. He is a fellow of the Optical Society, a member of the International Society for Optical Engineering and the Australian Optical Society. He was the recipient of the Croucher Senior Research Fellowship for 2000–2001and also the recipient of Japanese Government Research Award in 1987–1988.

Limin Xiao received the Ph.D. degree from the Hong Kong Polytechnic University in 2008. He is currently a Professor with the Advanced Fiber Devices and Systems Group, Key Laboratory of Micro and Nano Photonic Structures (MoE), Key Laboratory for Information Science of Electromagnetic Waves (MoE), Shanghai Engineering Research Center of Ultra-Precision Optical Manufacturing, School of Information Science and Technology, Fudan University, Shanghai, China. He currently heads the Advanced Fiber Devices and Systems Group. His research interests include photonic crystal fibers and devices, advanced optical fiber manufacturing technology, fiber sensors, all-fiber devices, and laser technology.